

Nonlinear behaviour of groundwater-surface water exchange flux

Moulshree Tripathi¹, Prabhas Kumar Yadav², Marc Walther³, Rudolf Liedl², B R Chahar⁴, and Peter Dietrich⁵

¹Indian Institute of Technology Delhi

²Technische Universität Dresden

³Helmholtz-Centre for Environmental Research (UFZ)

⁴Indian Institute of Technology

⁵UFZ, Helmholtz Centre for Environmental Research

November 22, 2022

Abstract

Understanding of the groundwater (GW)-surface water (SW) interaction is essential for the both qualitative and quantitative determination of the exchanging flux between them. The commonly used conductance-based approach, which linearly relates the flux with the streambed conductance, avoids the inclusion of aquifer properties in the flux quantification. In this approach, aquifer properties are solely represented by a hydraulic head below the streambed. Applying an analytical approach to a superimposed GW-SW system, this work finds that the exchanging flux rather follows a nonlinear behaviour when aquifer properties are part of flux quantification. The developed approach is found to match the numerical results obtained from synthetic data. The study further provides approaches for simpler quantification of geometrical and hydraulic properties of the streambed and the aquifer.

1 **Nonlinear behaviour of groundwater-surface water exchange flux**

2 **M. Tripathi^{1,2}, P. K. Yadav³, M. Walther^{4,5}, R. Liedl³, B. R. Chahar¹, and P. Dietrich²**

3 ¹Indian Institute of Technology, Department of Civil Engineering, Delhi, India

4 ²Helmholtz Centre for Environmental Research GmbH – UFZ, Department of Monitoring and
5 Exploration Technology, Leipzig, Germany

6 ³Technische Universität Dresden, Faculty of Environmental Sciences, Department of
7 Hydrosiences, Institute for Groundwater Management, Professorship of Groundwater
8 Management

9 ⁴Technische Universität Dresden, Faculty of Environmental Sciences, Department of
10 Hydrosiences, Institute for Groundwater Management, Professorship for Contaminant
11 Hydrology

12 ⁵Helmholtz Centre for Environmental Research GmbH – UFZ, Department of Environmental
13 Informatics, Leipzig, Germany

14 **Corresponding author:** Moulshree Tripathi (t.moulshree@gmail.com)

15 **Key Points:**

- 16 1. Developed an analytical approach to quantify GW-SW exchanging flux and to highlight
17 the significance of underlying aquifer.
- 18 2. The exchanging flux follows a nonlinear behaviour when aquifer properties are part of
19 flux quantification.
- 20 3. Provided a simpler approach to determine streambed specific conductance.

21

22

23 **Abstract**

24 Understanding of the groundwater (GW)-surface water (SW) interaction is essential for the both
25 qualitative and quantitative determination of the exchanging flux between them. The commonly
26 used conductance-based approach, which linearly relates the flux with the streambed
27 conductance, avoids the inclusion of aquifer properties in the flux quantification. In this
28 approach, aquifer properties are solely represented by a hydraulic head below the streambed.
29 Applying an analytical approach to a superimposed GW-SW system, this work finds that the
30 exchanging flux rather follows a nonlinear behaviour when aquifer properties are part of flux
31 quantification. The developed approach is found to match the numerical results obtained from
32 synthetic data. The study further provides approaches for simpler quantification of geometrical
33 and hydraulic properties of the streambed and the aquifer.

34 **Keywords:** Stream-aquifer interaction, parameter estimation, analytical approach, numerical
35 modelling

36 **1 Introduction**

37 The interactions between groundwater (GW) and the surface water (SW), the two major
38 components of the hydrological cycle, have great significance for the nutrient transport (Bencala,
39 2005), for maintaining riparian ecology (Boulton et al., 1998) and several other ecological
40 functions (Brunner et al., 2017). Compared to initial studies, these two components are now
41 widely recognised and researched as a single hydrological unit (Malard et al., 2002; McLachlan
42 et al., 2017). Its high ecological significance has increased the interest in GW-SW interaction
43 modelling (Boano et al., 2014; Brunner et al., 2017). It is now well established that the
44 interactions are mostly controlled by the two major components of the stream-aquifer system – a)
45 streambed and b) aquifer beneath the streambed (Alzraiee et al., 2017; Cardenas et al., 2004).

46 A streambed with respect to GW-SW interactions can be defined as an interface between the
47 stream and the aquifer. Studies such as Frei et al., (2009), Kalbus et al., (2009), Vogt et al.,
48 (2010) suggest that depending on the scale of the study, the hydrological properties (hydraulic
49 conductivity, porosity etc.), the geometrical properties (streambed width and thickness) and the
50 bedforms, of the streambed governs the GW-SW exchange. Among these, the hydraulic

51 conductivity of the streambed (K_r) has been suggested (e.g. Tang et al., 2017) to be the most
52 crucial parameter and a thorough knowledge of its spatial distribution is required for appropriate
53 estimation of GW-SW flux. However, the investigation of the spatial distribution K_r is a
54 challenging task, largely because of complexities of geological structures (Benoit et al., 2019).
55 The streambed thickness is another important parameter that significantly influences this
56 exchange. Field estimation of the streambed thickness is extremely difficult and it is generally
57 considered amongst a calibrating quantity in the modeling studies (e.g. CRIV in RIV Package,
58 MODFLOW, McDonald & Harbaugh, 1988).

59 The hydraulic conductivity of the aquifer (K_a), beneath the streambed, and its thickness are the
60 two significant quantities that guide the interactions through the streambed (Kalbus et al., 2009).
61 However, only very few modelling studies have tried to incorporate and model the influence of
62 aquifer beneath the streambed (e.g., Cousquer et al., 2017; Ghysels et al., 2019) to quantify GW-
63 SW interaction. The clear understanding of the overall nature of GW-SW interactions requires a
64 thorough understanding of the processes and reliable estimation of the flux across the stream
65 bed.

66 Numerical modelling approaches (e.g., RIV package of MODFLOW) utilising the linear
67 relationship between the flux and head-gradient, a so-called conductance-based approach, is
68 most commonly used for estimating GW-SW flux (e.g. Brunner et al., 2010; Ghysels et al., 2019;
69 Gooseff et al., 2006). The linear relation provides a possibility of infinitely increasing flux,
70 which may not always be practical.

71 In general, research works such as Brunner et al., (2010) considers the head difference between
72 the stream head and the head in the cell (or in the underlying aquifer) in which the stream is
73 modelled for quantifying the exchanges. As per this approach if the head in the aquifer
74 ($h_{aquifer}$) falls below the streambed bottom, the head in streambed bottom (h_{rbot}) replaces
75 $h_{aquifer}$ (e.g. RIV Package of MODFLOW). In practical cases, the streambed thickness may
76 vary in a range from few millimetres to few centimetres, and can significantly influence the head
77 drop and the vertical hydraulic gradient below the streambed. This leads to high uncertainties in
78 the determination of the streambed bottom or the thickness of colmation layer, and hence

79 increases the challenge with accurate quantification of h_{rbot} . To alleviate the challenge, this
 80 study proposes that $h_{aquifer}$ be measured at a certain distance from the stream.

81 The conductance of the streambed is a lumped parameter, consisting of the hydraulic as well as
 82 the geometrical properties of the streambed (e.g., Ghysels et al., 2019). The uncertainties
 83 involved in the quantification of the hydraulic conductivity, the width of the stream and the
 84 streambed thickness are extensively documented in works of Brunner et al., (2010), Ghysels et
 85 al., (2019). In addition, the accurate determination of hydraulic gradient in or below the
 86 streambed also poses a significant challenge, as the gradients may vary over a very short distance
 87 (Cremeans & Devlin, 2017).

88 Utilising mathematical approaches (analytical and numerical) this paper aims to study the
 89 contribution of the stream and the underlying aquifer on the flux and the resulting behaviour of
 90 the exchanging flux. The study develops an analytical approach to quantify the GW-SW flux
 91 from a 2D, two-component (streambed-aquifer) model setup. The behaviour of the flux through
 92 the developed analytical model is compared with a general numerical model using synthetic data.
 93 Finally, the significance of the developed approach and the properties of the underlying aquifer
 94 is highlighted.

95 **2. Approach**

96 The approach conceptualises a system with two components, a stream and an aquifer separated
 97 by a colmation layer (see Fig. 1). There exist two flows: (1) the vertical flow through the
 98 streambed and (2) the horizontal groundwater flow. The combined stream-aquifer system of this
 99 study represents the superposition of the horizontal groundwater flow and the vertical flow
 100 through the streambed. The superimposed system provides the flexibility to compute the flux
 101 through streambed separately and then incorporate the effect of it to the groundwater flow. For
 102 the conceptual development, we assume flow only through the streambed, i.e. without the
 103 groundwater flow. Further, the system is assumed to be homogenous, saturated and in a steady-
 104 state. In this setup (Fig. 1), $K_a [L/T]$, $W_a [L]$, and $t_a [L]$ define the aquifer properties,
 105 representing the hydraulic conductivity, width and thickness, respectively. $Q_r [L^2/T]$ is the flux
 106 through the streambed. $Q_{rr} [L^2/T]$ and $Q_{rl} [L^2/T]$ are the integrated fluxes at the aquifer
 107 boundary, involving stream infiltration on the right and the left side, respectively. $D [L]$

$$Q_r = K_r W_r \left(\frac{h_r - h_{int}}{t_r} \right) \quad (2)$$

127 Correspondingly, the flux (Q_{rl} and Q_{rr}) at either aquifer boundary can be expressed as the
 128 horizontal flux through the aquifer occurring due to the head gradient between the streambed
 129 bottom and the respective edge of the domain leading to

$$K_a t_a \left(\frac{h_{int} - h_a}{D + t_a + W_r/2} \right) < Q_{rl} < K_a t_a \left(\frac{h_{int} - h_a}{D} \right) \quad (3)$$

130 where the lower and the upper limits of the flux (at the left boundary in eq. 3) depends on the
 131 minimum (D) and maximum ($D + t_a + W_r/2$) distances for the gradient calculation,
 132 respectively. These distances are defined by the shortest and the longest streamline in the system
 133 (see Fig. 1). Eq. (3) thus incorporates both extremes of Q_{rl} . The symmetry of the setup will lead
 134 to identical expression as eq. (3) for Q_{rr} . Subsequent expressions will inherit the same ranges of
 135 fluxes as defined by eq (3).

136 As stated in the introductory section, h_{int} is subject to several challenges associated with its
 137 quantification, and hence we intend to replace it. From eq. (2) h_{int} can be obtained as

$$h_{int} = h_r - \frac{Q_r t_r}{K_r W_r} \quad (4)$$

138 Replacing h_{int} in eq. (3) from eq. (4) results to the following expression for flux at the aquifer
 139 boundary

$$K_a t_a \left(\frac{(h_r - Q_r t_r / K_r W_r) - h_a}{D + t_a + W_r / 2} \right) < Q_{rl} < K_a t_a \left(\frac{h_r - Q_r t_r / K_r W_r - h_a}{D} \right) \quad (5)$$

140 which can be rearranged as

$$\frac{Q_{rl} D}{K_a t_a} + \frac{Q_r t_r}{K_r W_r} < h_r - h_a < \frac{Q_{rl} (D + t_a + W_r / 2)}{K_a t_a} + \frac{Q_r t_r}{K_r W_r} \quad (6)$$

141 The symmetry of the setup and the constant head boundaries at the aquifer distributes the
 142 infiltrating stream flux equally to the edge of the aquifer. Therefore, the flux at the left and the
 143 right boundary will be

$$Q_{rl} = Q_r / 2 \quad (7a)$$

$$Q_{rr} = -Q_r / 2 \quad (7b)$$

144 The negative sign in eq. (7b) represents the opposite direction of the flow. Substituting Q_{rl} from
 145 eq. (7a) in eq. (6) and solving for Q_r we get

$$\frac{\frac{\Delta h}{(D+W_r/2+t_a)} + \frac{t_r}{K_r W_r}}{2K_a t_a} < Q_r < \frac{\frac{\Delta h}{D} + \frac{t_r}{K_r W_r}}{2K_a t_a} \quad (8)$$

146 Eq. (8) relates exchange flux with the hydraulic and geometrical properties of the streambed and
 147 the aquifer below it. Now, introducing the term specific conductance, C_r as

$$K_r/t_r = C_r \quad (9)$$

148 Unlike in eq. (1), the specific conductance in eq. (8), groups the parameters K_r and t_r , which
 149 generally are not quantified directly and, excludes W_r , which is easily determined. After some
 150 rearrangements (of eq. 8), the following expression for the stream infiltration is obtained

$$C_r W_r \left(\frac{\frac{\Delta h}{1 + \frac{C_r W_r (D+t_a+W_r/2)}}{2K_a t_a}} \right) < Q_r < C_r W_r \left(\frac{\frac{\Delta h}{1 + \frac{C_r W_r D}}{2K_a t_a}} \right) \quad (10)$$

151 The Q_r thus obtained avoids the uncertainties associated with quantifying h_{int} as suggested in
 152 Cremeans & Devlin, (2017). Eq. (10) in contrast to eq. (1), seems to have a nonlinear relation of
 153 flux with streambed and aquifer parameters. This is in contrast to a widely used linear approach
 154 (e.g. RIV package). The nonlinear behaviour of the flux is explored in the next section.

155 3. Behaviour of the flux

156 The presented analytical approach (eq. 10) seems to behave non-linearly with respect to
 157 streambed and aquifer properties. The further analysis of the nonlinear behaviour is performed
 158 using the conceptualised model setup in Fig 1 with parameters - $W_a = 45 \text{ m}$, $W_r = 15 \text{ m}$,
 159 $\Delta h = 0.1 \text{ m}$, $K_a = 1E - 4 \text{ m/s}$ and $t_a = 10 \text{ m}$. The specific conductance C_r being a critical
 160 parameter for direct quantification is used to compare the flux (Fig. 2). The C_r values are
 161 calculated by varying K_r ($1E - 6 \text{ m/s}$ to $1E - 4 \text{ m/s}$) and t_r (0.01 m to 0.75 m). Figure 2
 162 represents the variation of flux with C_r . The curve appears to follow a logistic curve with both
 163 the extremus and thus clearly nonlinear. The flux tends to become constant after a certain value
 164 of C_r ($1E-4$ for the above-described setup), which restricts flux to a certain maximum depending

165 upon the hydraulic and geometrical properties of the streambed and the aquifer. However, in eq.
 166 (1), the flux increases by increasing the C_r . This indicates a large overestimation of flux obtained
 167 using eq. (1). Furthermore, from eqs. (1) and (10), the head difference corresponds to the slope
 168 of the two approaches, subject to the condition when specific conductance tends to 0. Owing to
 169 this condition, the overlap between the two curves is restricted to a very small region.

170 Limited by the availability of field and lab data, the study further extends to examine the
 171 nonlinear behaviour using the synthetic numerical experiment of the above-conceptualised setup.

172 **3.1. Numerical example**

173 An identical numerical domain is setup using the same model dimensions that were used as in
 174 section 3. Further, the model includes all the assumptions made above for the development of the
 175 concept presented in eq. (10). In the numerical domain, the Dirichlet boundary (left and right 0
 176 and stream head = 0.1) is applied at the infiltrating stream and at the edge of the domain. The
 177 aquifer bottom in the setup is the no-flow boundary. The Gmsh mesh generator (Geuzaine &
 178 Remacle, 2017) was utilised for the finite element discretisation of the model domain, and an
 179 optimal mesh size was determined as smaller elements near the streambed (0.3) and larger near
 180 the aquifer boundaries (0.5). Scenarios were simulated using the open-source Groundwater_Flow
 181 module of numerical modelling tool OpenGeoSys v6.1 (www.opengeosys.org). The tool uses a
 182 linear homogeneous elliptic equation

$$div(k grad h) = 0 \text{ in } \Omega \quad (11)$$

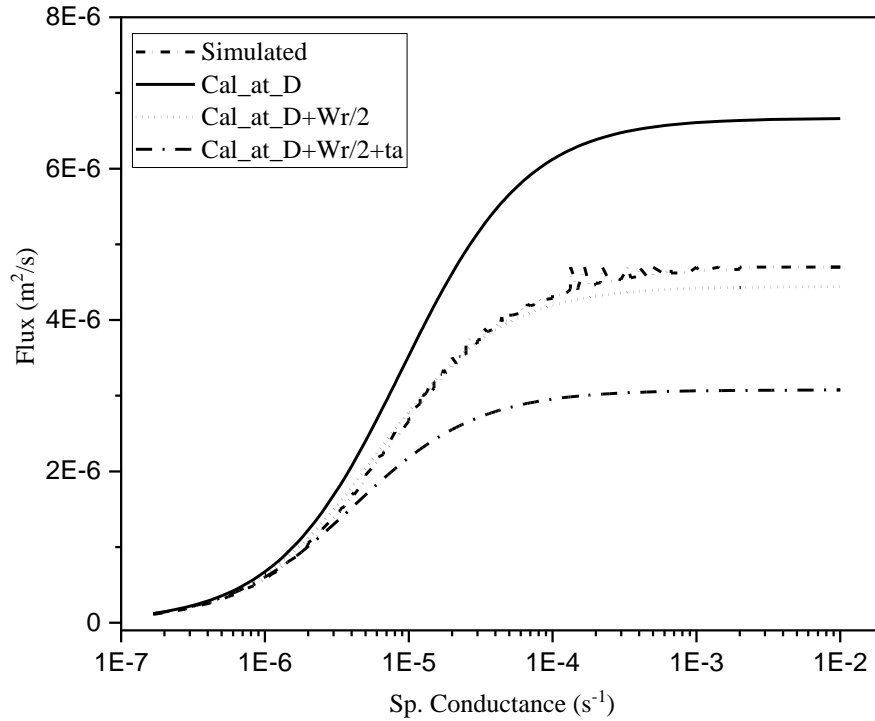
183 with respect to boundary conditions

$$184 \quad h(x) = g_D(x) \text{ on } \Gamma_D, \quad \frac{k \partial h(x)}{\partial n} = g_N(x) \text{ on } \Gamma_N,$$

185 where h is the hydraulic head, D and N denote the Dirichlet- and Neumann-type boundary
 186 conditions n represent normal vector pointing outside of Ω , and $\Gamma = \Gamma_D \cup \Gamma_N$ and $\Gamma_D \cap \Gamma_N = \emptyset$
 187 (further details can be obtained from:

188 <https://www.opengeosys.org/docs/benchmarks/elliptic/elliptic-dirichlet/>).

189 Figure 2 presents the results of numerical simulations. In the figure both the calculated and the
 190 simulated fluxes from different scenarios (varying K_r and t_r), are compared with respect to the
 191 specific conductance (C_r). As can be observed, the simulated results follow the same trend and
 192 lie between the calculated fluxes for both the limits resulting from eq. (10).



193

194 Figure 2: Comparison between the numerically obtained flux with that obtained using the
 195 developed analytical approach for three different streamlines.

196 Further, from eq. (7a) the simulated flux at any aquifer boundary will be half the magnitude of
 197 the calculated flux from eq. (10). The significant variation in the calculated flux magnitude is
 198 observed with the selection of the following three different distances: (1) at $D = (W_a - W_r)/2$;
 199 (2) at $D + t_a + W_r/2 = W_a/2 + t_a$ and (3) at $D + W_r/2 = W_a + W_r/2$ (Fig. 2). These three
 200 curves correspond to the effect of the gradients on the flux referring to the location of head
 201 measurements. The simulated curve is calculated at distance $D + W_r/2$, where $D < (W_a -$
 202 $W_r)/2$, and represents the case between cases 1 and 2 mentioned above. The distance in the
 203 simulated scenario is close to case 3, and hence the difference between the two curves is smaller
 204 than the curve for cases 1 and 2. The influence of hydraulic gradients is observed to be greater at
 205 higher specific conductance ($>10^{-5} \text{ s}^{-1}$). On the other hand, all four curves have insignificant

206 differences in flux at lower specific conductance ($<10^{-6} \text{ s}^{-1}$). The fluxes are found to be reaching
207 a maximum at higher specific conductance (10^{-3} s^{-1}). The calculated and the simulated curves
208 agree with the nonlinear behaviour of the flux with respect to the conductance and hence
209 contradicts the linear behaviour of the flux. The curves have minimum flux at a lower C_r value
210 and maximum at a higher C_r value.

211 Beyond the maximum specific conductance, the system tends to be governed by the aquifer
212 properties (see Fig. 2). The behaviour is in line with the physical system, i.e., where the
213 conductance of streambed is greater than the aquifer hydraulic conductivity, the flux determined
214 in the aquifer will be governed by the aquifer properties and not by the streambed conductance.
215 This limits the application of eq. (1) where the flux is based only on the streambed properties.
216 The developed approach hence can be considered as a more suitable approach towards the
217 exchange estimation as compared to the conductance-based approach when aquifer properties are
218 to be included as part of the model development. The value of the flux ranges between the
219 mentioned two cases and also verifies the assumption made in eq. (3). This assumption holds
220 true for different simulated scenarios (not presented in this work).

221 **4. Significance of the approach**

222 **4.1 Significance of the aquifer properties**

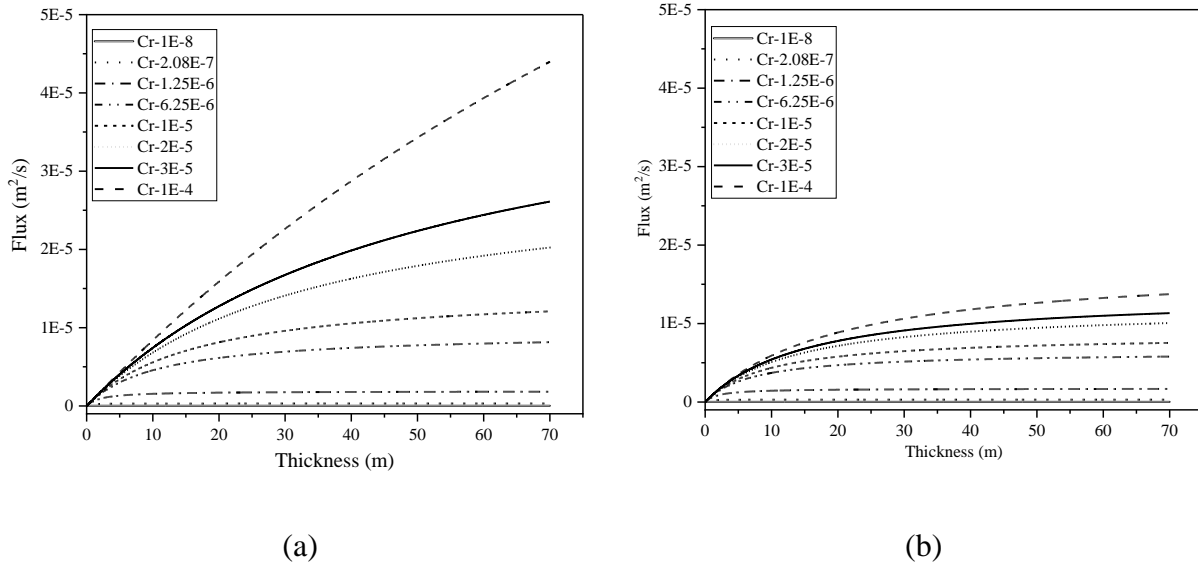
223 The developed approach in this work strongly emphasises on the incorporation of aquifer
224 properties for the quantification of the exchange flux. Based on the discussion in the previous
225 sections, the $h_{aquifer}$ is either measured beneath the stream bed or is replaced with h_{rbot} . If
226 considering the field measurements of the head beneath the streambed, in an ideal case, the
227 measurement should be done at the interface of the streambed bottom and the aquifer. However,
228 due to uncertainties involved in the delineation of the streambed and its varying thickness, the
229 head measurements are either in the streambed or at a certain depth in the aquifer. In the latter
230 case, the measured head has an influence of both streambed and the aquifer. The hydraulic
231 properties of the aquifer, as well as the geometry (mainly the thickness) of the aquifer, have a
232 significant impact on the head drop between the streambed bottom and the point of measurement
233 in the aquifer. This section illustrates the impact of these properties on the exchange
234 quantification.

235 The proposed expression (eq. 10) includes the thickness and the hydraulic conductivity of the
236 aquifer and the width of the streambed. The width of the aquifer, in the current study, represents
237 the extent of the aquifer at which head and flux measurements are to be done (see Fig. 1). This
238 section hence focuses on the influence of the thickness and the hydraulic conductivity of the
239 aquifer. For the illustration, the aquifer thickness and the hydraulic conductivity with a different
240 specific conductance of the streambed are varied, and obtained results are subsequently
241 discussed.

242 **4.1.1 Thickness of the aquifer**

243 In a natural stream-aquifer system, the aquifer can be a shallow or a deep aquifer or within these
244 two extremes. Considering eq. (10), the aquifer thickness defines the longest and the shortest
245 streamlines for exchange quantification. These streamlines have a significant effect when the
246 aquifer is shallow. To further illustrate the significance, eight specific conductance with
247 minimum $1\text{E-}8$ (s^{-1}) to maximum $1\text{E-}4$ (s^{-1}) were chosen depending on the minimum and
248 maximum for the value of K_r (between $1\text{E-}6$ m/s and $1\text{E-}4$ m/s) and t_r (between 0.01 m to 0.75
249 m).

250 Figures 3a and 3b represent the variation in the thickness over a minimum aquifer thickness to a
251 maximum aquifer thickness. The different curves tend to attain a constant value at a small
252 aquifer thickness for a given specific conductance. The two plots signify the incorporation of the
253 term t_a on eq. (10). For the specific conductance in the range of $1\text{E-}6$ s^{-1} to $1\text{E-}5$ s^{-1} , shallow
254 aquifer shows much variation in flux than the deeper ones. Hence, t_a should be part of the flux
255 estimation process especially for the shallow aquifers.

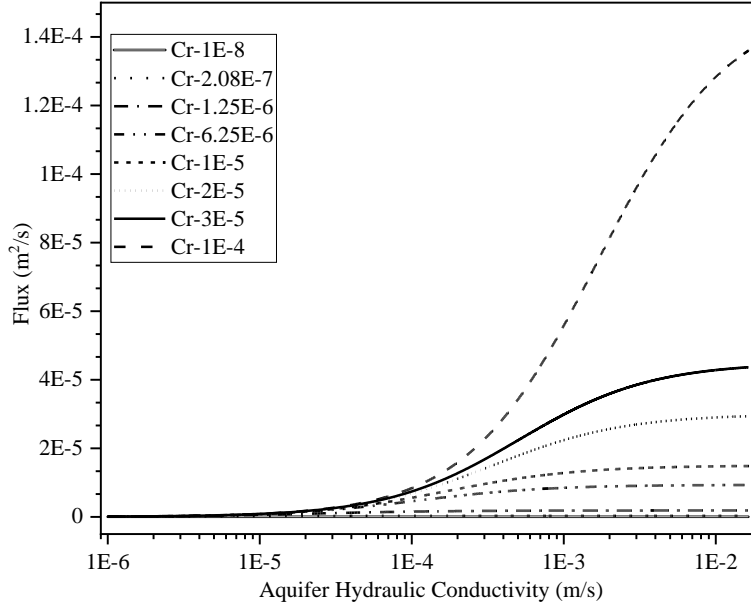


256 Figure 3: Effect of aquifer thickness with varying specific conductance of the streambed at a (a)
 257 distance $D + W_r/2$ (b) distance $D + W_r/2 + t_a$.

258 4.1.2 Hydraulic Conductivity of aquifer

259 The hydraulic conductivity of the aquifer (K_a) is another quantity that can significantly influence
 260 the GW-SW flux estimation to illustrate this, analysis of eq. (10) is considered using the setup
 261 similar to that used for specific conductance analysis (see section 4.1.1).

262 Based on Fig. 3, $t_a = 15$ m was considered an appropriate aquifer thickness for analysing the
 263 effect of K_a on GW-SW flux. Figure 4 demonstrates the behaviour of the hydraulic conductivity
 264 of the aquifer on the interacting flux. The behaviour is very similar to the behaviour of thickness
 265 with varying specific conductance C_r . This implies that for a very small value of K_a flux is
 266 independent of the specific conductance and is only governed by the K_a ($1E-6$ m/s). However,
 267 for very high values of K_a ($>1E-3$ m/s), the flux becomes constant and is dependent only on the
 268 specific conductance of the streambed. This analysis provides the range of K_a and the
 269 dependency of the flux on that range.



270

271 Figure 4: Effect of aquifer conductivity with varying specific conductance of the streambed

272 **4.2 Determination of Specific Conductance C_r**

273 Eq. (10) presents a straightforward method for the determination of GW-SW exchange flux. This
 274 approach can further be extended for the estimation of other streambed quantities. As already
 275 discussed, the conductance or the hydraulic conductivity of the streambed (C_r) is the most
 276 critical parameter in the determination of GW-SW exchanges. Also, in numerical modelling,
 277 estimating its magnitude is among the most challenging tasks. The details below utilise eq. (8)
 278 eq. (10) to provide an approach to easily obtain C_r .

279 First, eq. (8) is modified by replacing the value of K_r/t_r from eq. (10), as

$$\frac{1}{C_r W_r} < \frac{\Delta h}{Q_r} - \frac{D}{2K_a t_a} < \frac{\Delta h}{Q_r} - \frac{(D+t_a+W_r/2)}{2K_a t_a} \quad (12)$$

280 Rearranging the above equation provides the expression for C_r as

$$\frac{2K_a t_a Q_r}{W_r(2K_a t_a \Delta h - Q_r D)} < C_r < \frac{2K_a t_a Q_r}{W_r(2K_a t_a \Delta h - Q_r(D + t_a + W_r/2))} \quad (13)$$

281 Eq. (13) defines C_r from five quantities: the aquifer conductivity and thickness ($K_a t_a$), the width
 282 of the streambed (W_r), measured head (Δh), the distance of head measurement (D or $D + t_a +$
 283 $W_r/2$) and the infiltrating flux (Q_r). These parameters can be measured directly in the field or
 284 can be obtained using indirect estimation techniques.

285 For example, W_r can either be measured with a meter tape when the width is small or using
 286 remote sensing based on photogrammetry technology (Javernick et al., 2014). Ground-based
 287 cameras are another technique to measure the width (see Leduc et al., 2018). Aquifer properties
 288 such as transmissivity are most widely determined using the pumping tests. A slug test can be
 289 used for the quick estimate for the aquifer properties. Among these parameters, the most critical
 290 parameter in eq. (13) is Q_r and its determination is crucial for the estimation of C_r . The sub-
 291 section below presents an approach to quantify it.

292 **Determination of Q_r**

293 There are several techniques for the direct measurement of the infiltrating flux through the
 294 streambed, e.g. seepage meters (Rosenberry et al., 2020). In addition to the direct measurement
 295 techniques, there are several indirect techniques to quantify the exchanging flux. Among these,
 296 the flux estimation using heat as the tracer is most common (Gordon et al., 2012; Lautz et al.,
 297 2010).

298 The above-mentioned techniques consider measurements in the stream, which is subjected to
 299 challenges including streamflow, alteration of the streambed hydraulic conductivity due to
 300 instrument installation, and is limited to point measurement of the data. These challenges can be
 301 overcome if we could estimate the infiltrating flux in the surrounding aquifer.

302 The GW-SW interaction system, as also considered in this work, can be treated as a
 303 superimposed system of groundwater flow and the stream infiltration (see Section 2). Therefore,
 304 the flux estimated at any aquifer boundary, i.e. the point of measurements on both sides of the
 305 stream (say right side flux be - Q_{ar} and left side flux be - Q_{al}) will have the influence of both

306 groundwater flow in the aquifer (Q_a) and the stream infiltration (Q_r). In a losing stream, the
 307 fluxes thus can be obtained from

$$Q_{al} = Q_a + Q_r/2 \quad (14a)$$

$$Q_{ar} = Q_a - Q_r/2 \quad (14b)$$

308 The Q_r in the eq. (14b) represents the opposite direction of contributing stream flux with respect
 309 to the groundwater flow in the aquifer. Subtracting eq. (14 b) from eq. (14 a) provides the
 310 following expression for Q_r :

$$Q_r = Q_{al} - Q_{ar} \quad (15)$$

311 The fluxes Q_{al} and Q_{ar} , can be estimated by measuring the head gradient on the left and the
 312 right side of the stream (as shown in Fig. 1). This method involves measurement of the stream
 313 stage and groundwater heads in a network of wells on both sides of the stream, to calculate
 314 gradients and then the exchanging flux. The method is suitable when the groundwater flow is
 315 lateral to the streamflow. However, the case of losing and gaining stream could be addressed
 316 using this approach by simply changing the direction of the flow.

317 **5. Conclusions and Outlook**

318 The conductance-based approach, a linear approach, requires modification for determining the
 319 stream-aquifer interaction. The approach involves challenges in the determination of hydraulic
 320 head below the streambed and the conductance of the streambed. The developed formulation
 321 provides a more logistic approach towards the determination of the GW-SW interaction by
 322 eliminating the uncertainties and challenges involved in the head measurement required below
 323 the streambed. This straightforward approach is extended for the development of the expression
 324 for the streambed parameter estimation. The formulated expression for the streambed flux and
 325 the streambed specific conductance holds for the different numerical simulations. These
 326 numerically verified expressions can further be tested using field measurements/data. The

327 exchange flux could either be quantified using the head measurement in the aquifer or direct
328 quantification of the flux using heat measurement techniques.

329 The GW-SW interaction is a very complex process, and hence a step-by-step model built up, and
330 process understanding is very necessary. The presented approach involves many assumptions.
331 However, the concept could be extended to address the more complex systems involving the
332 asymmetric stream-aquifer system and varying the hydraulic head along the edge of the aquifer.
333 In a natural stream-aquifer system, the orientation of the groundwater flow could be along the
334 streamflow, lateral to the stream or flowing at some angle to the direction of streamflow. These
335 issues could be addressed by extending to the 3-dimensional model.

336 **Acknowledgements**

337 The work was partially funded by Deutscher Akademischer Austauschdienst (DAAD) (*Research*
338 *Grants – Bi-nationally Supervised Doctoral Degrees*), and Ministry of Human Resources
339 Development, India. The development of the presented work did not use any data, nor created
340 any dataset. Parameter values and ranges have been used for the development of the curves and
341 are already cited in the text above.

342 **References**

- 343 Alzraiee, A. H., Bailey, R., & Bau, D. (2017). Assimilation of historical head data to estimate
344 spatial distributions of stream bed and aquifer hydraulic conductivity fields. *Hydrological
345 Processes*, 31(7), 1527–1538. <https://doi.org/10.1002/hyp.11123>
- 346 Bencala, K. E. (2005). Hyporheic exchange flows. *Encyclopedia of Hydrological Sciences*,
347 (APRIL 2006), 1–7. <https://doi.org/10.1002/0470848944.hsa126>
- 348 Benoit, S., Ghysels, G., Gommers, K., Hermans, T., Nguyen, F., & Huysmans, M. (2019).
349 Characterisation of spatially variable riverbed hydraulic conductivity using electrical
350 resistivity tomography and induced polarisation. *Hydrogeology Journal*, 27(1), 395–407.
351 <https://doi.org/10.1007/s10040-018-1862-7>
- 352 Boano, F., Harvey, J. W., Marion, A., Packman, A. I., Revelli, R., Ridolfi, L., & Wörman, A.
353 (2014). Hyporheic flow and transport processes: Mechanisms, models, and biogeochemical
354 implications. *Reviews of Geophysics*, 52(4), 603–679.
355 <https://doi.org/10.1002/2012RG000417>
- 356 Boulton, A. J., Findlay, S., Marmonier, P., Stanley, E. H., & Valett, H. M. (1998). THE
357 FUNCTIONAL SIGNIFICANCE OF THE HYPORHEIC ZONE IN STREAMS AND
358 RIVERS. *Annu. Rev. Ecol. Syst.*, 29, 59–81.
- 359 Brunner, P., Simmons, C. T., Cook, P. G., & Therrien, R. (2010). Modeling surface water-
360 groundwater interaction with MODFLOW: Some considerations. *Ground Water*, 48(2),
361 174–180. <https://doi.org/10.1111/j.1745-6584.2009.00644.x>
- 362 Brunner, P., Therrien, R., Renard, P., Simmons, C. T., & Franssen, H. J. H. (2017). Advances in
363 understanding river-groundwater interactions. *Reviews of Geophysics*, 55(3), 818–854.
364 <https://doi.org/10.1002/2017RG000556>
- 365 Cardenas, M. B., Wilson, J. L., & Zlotnik, V. A. (2004). Impact of heterogeneity, bed forms, and
366 stream curvature on subchannel hyporheic exchange. *Water Resources Research*, 40(8), 1–
367 14. <https://doi.org/10.1029/2004WR003008>

- 368 Cousquer, Y., Pryet, A., Flipo, N., Delbart, C., & Dupuy, A. (2017). Estimating River
 369 Conductance from Prior Information to Improve Surface-Subsurface Model Calibration.
 370 *Groundwater*, 55(3), 408–418. <https://doi.org/10.1111/gwat.12492>
- 371 Cremeans, M. M., & Devlin, J. F. (2017). Validation of a new device to quantify groundwater-
 372 surface water exchange. *Journal of Contaminant Hydrology*, 206, 75–80.
 373 <https://doi.org/10.1016/j.jconhyd.2017.08.005>
- 374 Frei, S., Fleckenstein, J. H., Kollet, S. J., & Maxwell, R. M. (2009). Patterns and dynamics of
 375 river-aquifer exchange with variably-saturated flow using a fully-coupled model. *Journal of*
 376 *Hydrology*, 375(3–4), 383–393. <https://doi.org/10.1016/j.jhydrol.2009.06.038>
- 377 Geuzaine, C., & Remacle, J.-F. (2017). A three-dimensional finite element mesh generator with
 378 built-in pre- and post-processing facilities. *Int. J. Numer. Meth. Engng.*, 79(11), 1309–1331.
 379 Retrieved from http://gmsh.info/doc/preprints/gmsh_paper_preprint.pdf
- 380 Ghysels, G., Mutua, S., Veliz, G. B., & Huysmans, M. (2019). A modified approach for
 381 modelling river–aquifer interaction of gaining rivers in MODFLOW, including riverbed
 382 heterogeneity and river bank seepage. *Hydrogeology Journal*, 1–13.
 383 <https://doi.org/10.1007/s10040-019-01941-0>
- 384 Gooseff, M. N., Anderson, J. K., Wondzell, S. M., LaNier, J., & Haggerty, R. (2006). A
 385 modelling study of hyporheic exchange pattern and the sequence, size, and spacing of
 386 stream bedforms in mountain stream networks, Oregon, USA. *Hydrological Processes*.
 387 <https://doi.org/10.1002/hyp.6349>
- 388 Gordon, R. P., Lautz, L. K., Briggs, M. A., & McKenzie, J. M. (2012). Automated calculation of
 389 vertical pore-water flux from field temperature time series using the VFLUX method and
 390 computer program. *Journal of Hydrology*, 420–421, 142–158.
 391 <https://doi.org/10.1016/j.jhydrol.2011.11.053>
- 392 Kalbus, E., Schmidt, C., Molson, J. W., Reinstorf, F., & Schirmer, M. (2009). Influence of
 393 aquifer and streambed heterogeneity on the distribution of groundwater discharge.
 394 *Hydrology and Earth System Sciences*, 13(1), 69–77. <https://doi.org/10.5194/hess-13-69->

- 395 2009
- 396 Lautz, L. K., Kranes, N. T., & Siegel, D. I. (2010). Heat tracing of heterogeneous hyporheic
397 exchange adjacent to in-stream geomorphic features. *Hydrological Processes*, 24(21),
398 3074–3086. <https://doi.org/10.1002/hyp.7723>
- 399 Leduc, P., Ashmore, P., & Sjogren, D. (2018). Technical note: Stage and water width
400 measurement of a mountain stream using a simple time-lapse camera. *Hydrology and Earth
401 System Sciences*, 22(1), 1–11. <https://doi.org/10.5194/hess-22-1-2018>
- 402 Malard, F., Tockner, K., Dole-Olivier, M.-J., & Ward, J. V. (2002). A landscape perspective of
403 surface-subsurface hydrological exchanges in river corridors. *Freshwater Biology*, 47(4),
404 621–640. <https://doi.org/10.1046/j.1365-2427.2002.00906.x>
- 405 McDonald, M. G., & Harbaugh, A. W. (1988). *A modular three-dimensional finite-difference
406 ground-water flow model. Techniques of Water-Resources Investigations.*
407 <https://doi.org/10.3133/twri06A1>
- 408 McLachlan, P. J., Chambers, J. E., Uhlemann, S. S., & Binley, A. (2017). Geophysical
409 characterisation of the groundwater–surface water interface. *Advances in Water Resources*,
410 109, 302–319. <https://doi.org/10.1016/j.advwatres.2017.09.016>
- 411 Rosenberry, D. O., Duque, C., & Lee, D. R. (2020, May 1). History and evolution of seepage
412 meters for quantifying flow between groundwater and surface water: Part 1 – Freshwater
413 settings. *Earth-Science Reviews*. Elsevier B.V.
414 <https://doi.org/10.1016/j.earscirev.2020.103167>
- 415 Tang, Q., Kurtz, W., Schilling, O. S., Brunner, P., Vereecken, H., & Hendricks Franssen, H. J.
416 (2017). The influence of riverbed heterogeneity patterns on river-aquifer exchange fluxes
417 under different connection regimes. *Journal of Hydrology*, 554, 383–396.
418 <https://doi.org/10.1016/j.jhydrol.2017.09.031>
- 419 Vogt, T., Schneider, P., Hahn-Woernle, L., & Cirpka, O. A. (2010). Estimation of seepage rates
420 in a losing stream by means of fiber-optic high-resolution vertical temperature profiling.
421 *Journal of Hydrology*, 380(1–2), 154–164. <https://doi.org/10.1016/j.jhydrol.2009.10.033>